A Technique for Avoiding the EFIE "Interior Resonance" Problem Applied to an MM Solution of Electromagnetic Radiation from Bodies of Revolution

Pierre Steyn and David B. Davidson

Department of Electrical and Electronic Engineering

University of Stellenbosch, Stellenbosch 7600, South Africa

e-mail: davidson@firga.sun.ac.za

Abstract

Various surface integral equation formulations, including the electric (EFIE) and magnetic (MFIE) field integral equations, suffer from what is commonly known as the "interior resonance" problem. There are a number of remedies to this problem of which many involve modifying the integral equation formulation and result in increased computational effort and computer storage requirements. In an attempt to avoid this the application of a remedy, proposed in the literature, which requires no modification to the formulation has been investigated. This involves the detection of interior resonance frequencies and correction of the current by removing the mode responsible for the "interior resonance". In the literature, the success of the remedy has been demonstrated for two-dimensional scattering problems involving PEC cylinders. In this work it is demonstrated that, while the correction of the MM (moment method) solution is successful when an "interior resonance" has been detected, the detection of the interior resonance frequencies can be extremely difficult in an MM solution of radiation from composite bodies of revolution. In fact, a foolproof computational algorithm for detecting interior resonance frequencies for this class of problems is yet to be developed.

1 Introduction

The electric field integral equation (EFIE) and magnetic field integral equation (MFIE) suffer from what is commonly known as the "interior resonance" problem. The reason for this is that some surface integral equation (SIE) formulations, including the EFIE and MFIE, can be used to represent both an interior and an exterior electromagnetic problem for a closed geometry. The exterior problem involves fields produced by an applied source whereas the interior, or cavity, problem involves source-free "resonant cavity modes". The cavity modes of the interior problem occur at discrete frequencies known as eigenfrequencies. Thus, when solving the exterior problem in the region of these eigenfrequencies, the SIE's solution is not unique because a nontrivial solution exists to the interior problem.

The problem is widely reported in the literature, e.g. [1, 2, 3, 4, 5]. Recently, Peterson presented an excellent review of the problem, along with a survey of various remedies [6]. Numerous references to the literature are included therein.

Many of the remedies to the problem involve modifying the SIE formulation. For example, the combined field integral equation (CFIE) [1], involving a linear combination of the EFIE and MFIE, yields unique solutions at all frequencies. These remedies require more computational effort than the EFIE or MFIE and possibly more computer storage as well.

A remedy proposed by Canning in [7] involves solving the EFIE or MFIE without modifications and correcting the solution near eigenfrequencies. Algorithms that execute this correction, which involves detecting the presence of a cavity mode superimposed on the desired solution and "discarding" it, can be added to existing MM solutions of the EFIE and MFIE without major modifications.

The purpose of the study presented here is to investigate the application of this method to an existing MM/BOR formulation for the solution of scattering [8] and radiation [9] from composite bodies of revolution[1].

[1] By composite it is meant here as made up of different homogeneous isotropic material regions, penetrable by electromagnetic waves, and perfectly electrically conducting regions surrounded by free space. The material regions can be lossy.

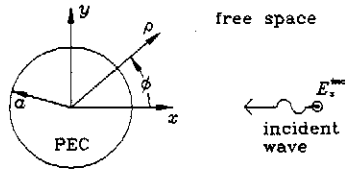

Figure 1: A circular cylinder of infinite length, extending from $z = -\infty$ to ∞ (the z-axis points out of the page), illuminated by a TM plane wave.

For conducting regions the MM/BOR formulation utilizes the EFIE, while for penetrable regions the CFIE is used.

Following this introduction is a demonstration of the "interior resonance" problem in the application of the EFIE to a two-dimensional problem. This is followed by a numerical investigation of the problem, which follows the work presented by Canning in [10] although from a different perspective, wherein the singular value decomposition (SVD) was used to demonstrate why the "interior resonance" problem occurs. The application of Canning's remedy to the canonical problems is then discussed. Finally, Canning's remedy is applied to the MM/BOR formulation and subtleties involved in its implementation are demonstrated and discussed.

2 Demonstration of the "Interior Resonance" problem

To illustrate the interior resonance problem it is useful to analyze a problem that can be solved analytically. Such a problem, which has previously been investigated by Peterson [6] and Canning [10], is scattering of a transverse magnetic (TM) plane wave from a perfectly electrically conducting (PEC) circular cylinder of infinite length. It is presented here in a different manner in order to highlight certain points. The problem is illustrated in Figure 1. Here the incident plane wave is assumed to be traveling in the negative x-direction with the incident electric field given by

$$\vec{E}^{inc} = \hat{z} E_0 e^{jk_0 x} \tag{1}$$

where E_0 is a constant, $\hat{z}$ is the unit vector in the z-direction and k_0 is the wave number of free space. This is a two-dimensional problem with the EFIE given by

$$\vec{E}^{inc}|_{\rho=a} = \hat{z}\frac{k_0 a \eta_0}{4}\int_{-\pi}^{\pi} J_z(\phi') H_0^{(2)}(k_0 a|\hat{\rho} - \hat{\rho}'|)\, d\phi' \tag{2}$$

where unprimed coordinates indicate the field point, primed coordinates the source point, a is the radius of the cylinder, and η_0 is the intrinsic impedance of free space. The kernel of the integral, $H_0^{(2)}$, is the Hankel function of the second type and order zero, and J_z is the desired surface current.

An MM solution to this problem will be compared with an analytical solution.

An analytical solution for the problem can be obtained by following the MM solution procedure [11, pages 5-6] as follows. The surface current is expanded as a Fourier series that is appropriate to the geometry of the problem, i.e.

$$J_z(\phi) = \frac{a_0}{2} + \sum_{n=1}^{\infty}(a_n \cos n\phi + b_n \sin n\phi) \tag{3}$$

where a_n and b_n are unknown coefficients. The expansion functions are $\{\frac{1}{2}, \cos n\phi, \sin n\phi\}$ with $n = 1, \ldots, \infty$, and the testing functions are chosen as $\{1, \cos m\phi, \sin m\phi\}$ with $m = 1, \ldots, \infty$. By substituting equation (3) into (2) and forming the inner product with each testing function, equation (2) is transformed into the infinite order matrix equation

$$\begin{bmatrix} \Lambda_0 & 0 & 0 & \cdots & 0 & 0 & \cdots & 0 & 0 \\ 0 & \Lambda_1 & 0 & \cdots & 0 & 0 & \cdots & 0 & 0 \\ 0 & 0 & \Lambda_1 & \cdots & 0 & 0 & \cdots & 0 & 0 \\ \vdots & \vdots & \vdots & \ddots & \vdots & \vdots & & \vdots & \vdots \\ 0 & 0 & 0 & \cdots & \Lambda_m & 0 & \cdots & 0 & 0 \\ 0 & 0 & 0 & \cdots & 0 & \Lambda_m & \cdots & 0 & 0 \\ \vdots & \vdots & \vdots & & \vdots & \vdots & \ddots & \vdots & \vdots \\ 0 & 0 & 0 & \cdots & 0 & 0 & \cdots & \Lambda_\infty & 0 \\ 0 & 0 & 0 & \cdots & 0 & 0 & \cdots & 0 & \Lambda_\infty \end{bmatrix} \begin{bmatrix} a_0 \\ a_1 \\ b_1 \\ \vdots \\ a_n \\ b_n \\ \vdots \\ a_\infty \\ b_\infty \end{bmatrix}$$

$$= \begin{bmatrix} \mathcal{V}_0 & \mathcal{V}_1 & 0 & \cdots & \mathcal{V}_m & 0 & \cdots & \mathcal{V}_\infty & 0 \end{bmatrix}^T \tag{4}$$

where $\mathcal{V}_n = 2E_0 j^n J_n(k_0 a)$, with J_n being the Bessel function of order n, and $\Lambda_0, \Lambda_1, \ldots, \Lambda_\infty$ are the eigenvalues of equation (2) which are given by

$$\Lambda_m = \frac{\eta_0 \pi k_0 a}{2} J_m(k_0 a) H_m^{(2)}(k_0 a) \tag{5}$$

where $H_m^{(2)}$ is the m-th order Hankel function of the second type.

Since the matrix of equation (4) is diagonal, the unknown coefficients can easily be obtained and are, for $n = 0, 1, \ldots, \infty$,

$$a_n = \frac{4E_0 j^n}{\eta_0 \pi k_0 a H_n^{(2)}(k_0 a)}, \tag{6}$$

$$b_n = 0. \tag{7}$$

The surface current can then be determined using equation (3) with these coefficients.

For a given $k_0 a$ value the magnitude of the coefficients of equation (6) decreases with increasing n and beyond about $n = k_0 a + 2\pi$ their magnitudes are less than one percent of a_0. Thus, $J_z(\phi)$ can be computed reasonably accurately using $N_{max} \geq k_0 a + 2\pi$ terms in the summation in equation (3).

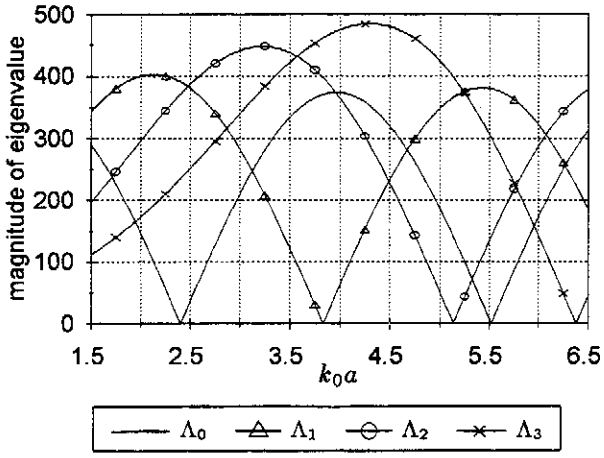

Figure 2: Behavior of the first few eigenvalues versus k_0a for a circular cylinder of infinite length.

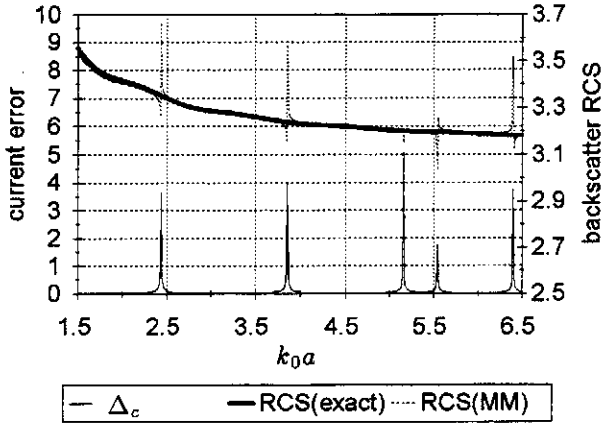

Figure 3: Electric current error Δ_C in the MM solution and backscatter RCS, exact and MM solutions, versus k_0a for scattering by a PEC circular cylinder of infinite length excited by an incident TM plane wave.

The interior problem, i.e. the circular cavity of infinite length formed by the outer boundary of the cylinder, described by equation (2) with the left hand side set to zero, has nontrivial solutions at frequencies where the eigenvalues of equation (5) are zero. These coincide with the zeros of $J_m(k_0a)$ with $m = 0, 1, \ldots, \infty$. The behaviour of the first few eigenvalues from $k_0a = 1.5$ to 6.5, computed using equation (5), are plotted in Figure 2. The first few resonances are seen to occur at $k_0a = 2.405$, 3.832, 5.136, 5.520 and 6.380 with the responsible eigenvalues being Λ_0, Λ_1, Λ_2, Λ_0, and Λ_3 respectively.

An approximate, but more general, MM solution to equation (2) was obtained using pulse basis functions and impulse testing functions as described in [11, pages 42-45]. The circle that generates the circular cylinder was approximated by a regular N-sided polygon, circumscribed by the circle. The pulses coincided with the sides of this polygon and the testing was done at the centres of these sides. The non-diagonal elements of the impedance matrix were found by approximating each integral by the value of the integrand at the middle of the pulse multiplied by the pulse width [11, equation (3-12)]. To avoid the singularity in the self terms, the diagonal elements were obtained by replacing the Hankel functions by their small argument form and integrating analytically [11, equation (3-14)]. The result is a matrix equation

$$\mathbf{ZJ} = \mathbf{E}_i \tag{8}$$

where the vector $\mathbf{J}$ contains the unknown current coefficients, the elements of $\mathbf{E}_i$ are given, with $E_0 = 1$, by

$$E_{im} = \Delta C_m e^{jk_0x_m} \tag{9}$$

and the elements of $\mathbf{Z}$ given by

$$Z_{mn} = \begin{cases} \frac{k_0\eta_0\Delta C_m\Delta C_n}{4} H_0^{(2)}[k_0\sqrt{(x_n-x_m)^2+(y_n-y_m)^2}] \\ \qquad\qquad m \neq n, \\ \frac{k_0\eta_0\Delta C_m\Delta C_n}{4}\left[1 - j\frac{2}{\pi}\log\left(\frac{\gamma k_0\Delta C_n}{4e}\right)\right] \\ \qquad\qquad m = n \end{cases} \tag{10}$$

where ΔC_m is the width of pulse m, x_m and y_m are the coordinates of the centre of pulse m, $\gamma = 1.7810724\ldots$ such that $\log\gamma$ is Euler's constant and $e = 2.7182818\ldots$ is the natural base of logarithms. Here the widths of all the pulses are equal which results in $\mathbf{Z}$ for this problem being complex symmetric (it is, in fact, Toeplitz).

The current, $\vec{J}_{MM}$, obtained using the formulas of equations (10) and (9) can be compared with the "exact" current, $\vec{J}_{exact}$, computed using equation (3) by determining the current error, Δ_C, given by [1, equation (30)]

$$\Delta_C = \sqrt{\frac{\iint_S |\vec{J}_{MM} - \vec{J}_{exact}|^2\, ds}{|\vec{H}^{inc}|^2 \iint_S ds}}. \tag{11}$$

where S is the surface of the PEC cylinder and $\vec{H}^{inc}$ is the incident magnetic field. A plot of Δ_C for this problem, from $k_0a = 1.5$ to 6.5, is given in Figure 3. The number of unknowns N_{MM} in the MM computation varied with k_0a according to the formula

$$N_{MM} \geq 10k_0a \tag{12}$$

which ensures that there are 10 unknowns per wavelength. It is observed that Δ_C is small except in the vicinity of those values of k_0a that coincide with the interior resonances observed in Figure 2.

Also plotted in Figure 3 is the backscatter radar cross section (RCS) computed by the exact solution and the MM which demonstrates that the anomalies in the current couple to the far field.

3 Investigation of the "Interior Resonance" problem using the SVD

Canning introduced the application of the SVD to the study of MM matrices in [10]. The SVD is discussed in numerous texts related to linear algebra, for example [12]. An SVD of an N-by-N matrix $\mathbf{A}$ is any factorization of the form

$$\mathbf{A} = \mathbf{USV}^h \tag{13}$$

where the superscript h indicates the Hermitian conjugate, $\mathbf{U}$ is an N-by-N unitary matrix, $\mathbf{V}$ is an N-by-N unitary matrix and $\mathbf{S}$ is an N-by-N diagonal matrix with elements $s_{mn} = 0$ if $m \neq n$. The diagonal elements of $\mathbf{S}$, $s_n = s_{nn}$, are known as the singular values. These are real, nonnegative and arranged in order of decreasing magnitude. The columns of $\mathbf{U}$ are the left singular vectors and the columns of $\mathbf{V}$ are the right singular vectors.

By following the MM procedure, the EFIE is transformed to a matrix equation of the form given by equation (8). Decomposition of $\mathbf{Z}$ to its SVD reduces equation (8) to the diagonal equation

$$\mathbf{S}\tilde{\mathbf{J}} = \tilde{\mathbf{E}}_i \tag{14}$$

where $\tilde{\mathbf{J}} = \mathbf{V}^h\mathbf{J}$ and $\tilde{\mathbf{E}}_i = \mathbf{U}^h\mathbf{E}_i$. Thus, the SVD diagonalizes the MM equation and $\tilde{\mathbf{J}}$ and $\tilde{\mathbf{E}}_i$ are the currents and fields expressed in the bases that diagonalize the problem – the columns of $\mathbf{V}$ and $\mathbf{U}$ respectively. The elements of $\tilde{\mathbf{J}}$, the coefficients of the diagonalizing current bases, are easily obtained by

$$\tilde{j}_m = \frac{\tilde{e}_m}{s_m} \tag{15}$$

where $\tilde{e}_m$ is the m-th element of $\tilde{\mathbf{E}}_i$.

The SVD can be used to reach an understanding of how the interior resonance problem occurs for the problem of scattering of a TM plane wave from a PEC circular cylinder of infinite length. For this particular problem, the singular values of $\mathbf{Z}$ are numerically equal to the magnitude of the eigenvalues of $\mathbf{Z}$ (this may be because the eigenvalues are approximately orthogonal). Thus, the singular values of the approximate MM matrix of order N_{MM} are approximations of the magnitudes of the first $\frac{N_{MM}}{2} + 1$ eigenvalues of equation (5) if N_{MM} is even, or the first $\frac{N_{MM}+1}{2}$ if N_{MM} is odd. This is demonstrated in Table 1 where the singular values are compared with the magnitudes of the exact eigenvalues for $k_0a = 1$ and $N_{MM} = 8$.

Singular values of MM solution	*Magnitudes of eigenvalues of exact solution*
$s_1 = 367.698$	$\lvert\Lambda_0\rvert = 348.796$
$s_2 = 219.017$	$\lvert\Lambda_1\rvert = 233.490$
$s_3 = 219.017$	$\lvert\Lambda_1\rvert = 233.490$
$s_4 = 102.139$	$\lvert\Lambda_2\rvert = 112.513$
$s_5 = 102.139$	$\lvert\Lambda_2\rvert = 112.513$
$s_6 = 65.500$	$\lvert\Lambda_3\rvert = 67.396$
$s_7 = 65.500$	$\lvert\Lambda_3\rvert = 67.396$
$s_8 = 57.423$	$\lvert\Lambda_4\rvert = 48.773$

Table 1: The singular values of $\mathbf{Z}$ and the magnitudes of the exact eigenvalues for the circular cavity of infinite length with $k_0a = 1$ and $N_{MM} = 8$.

Further, the columns of $\mathbf{U}$ and $\mathbf{V}$ are approximations of the basis functions of the exact solution, i.e. $\{\frac{1}{2}, \cos n\phi, \sin n\phi\}$. This is demonstrated in Table I of [10] for $k_0a = 1$ and $N_{MM} = 8$.

Thus, the resonance problem should occur whenever the smallest singular value $s_{N_{MM}}$ approaches zero. This is verified in Figure 4 where $s_{N_{MM}}$ is plotted for $k_0a = 1.5$ to 6.5. In the vicinity of a value of k_0a which corresponds to an interior resonance, $s_{N_{MM}}$ is observed to tend rapidly to zero since it corresponds to the eigenvalue responsible for the resonance. Otherwise, away from interior resonances where it corresponds to the eigenvalue with largest index (away from a resonance, for a given value of k_0a, the eigenvalues decrease in magnitude with increasing index), $s_{N_{MM}}$ remains almost constant with increasing k_0a .

Equations (4) to (6) provide a clue as to how the interior resonance problem occurs. In computing the coefficient a_n in the exact solution, the Bessel function, $J_n(k_0a)$, that is present in the eigenvalue Λ_n cancels out as it also occurs in the excitation. It is this factor that becomes zero at an interior resonance making the corresponding eigenvalue zero. Thus it is not present in the exact solution for the exterior problem. However, the discretization error perturbs the MM matrix eigenvalue from the exact eigenvalue [6] and in the vicinity of an interior resonance numerical instability can be expected if the factor in the eigenvalue does not cancel properly with the factor in the excitation.

Using the SVD, the MM matrix equation is diagonal-

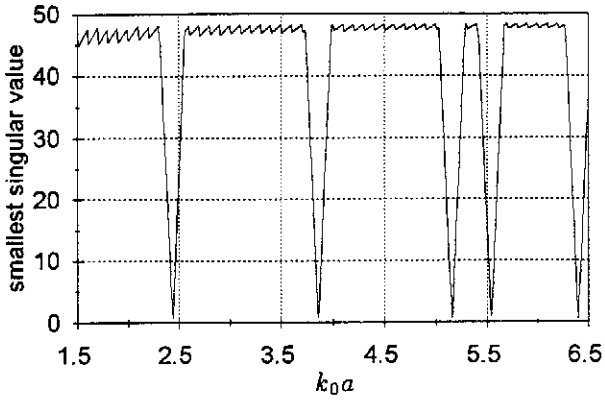

Figure 4: Smallest singular value $s_{N_{MM}}$, versus k_0a, of the MM impedance matrix for a PEC circular cylinder of infinite length.

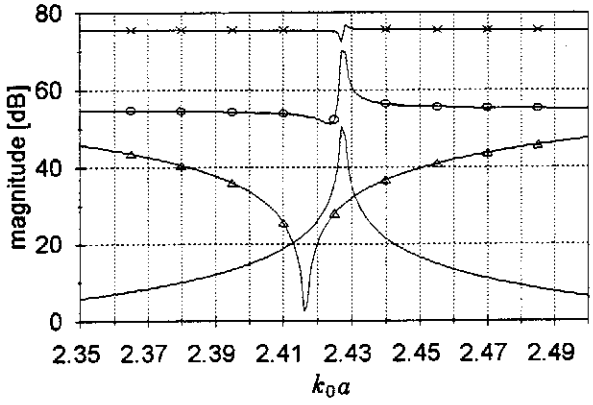

Figure 5: Behavior, in the vicinity of the lowest interior resonance, of the inverse of the smallest singular value $s^{-1}_{N_{MM}}$, the measure of the cavity mode excitation $\tilde{e}_{N_{MM}}$, the current on the near side of the incoming plane wave J_1 and the backscatter RCS σ versus k_0a in the MM solution of scattering by a circular cylinder of infinite length excited by an incident TM plane wave with $N_{MM} = 32$. The curves are vertically shifted from each other for clarity and 0 dB is arbitrary.

ized to the form of equation (14). In this form, the coefficients in the diagonalized current vector $\tilde{\mathbf{J}}$ are easily obtained using equation (15). However, in the vicinity of a resonance, $s_{N_{MM}}$ tends toward zero and one can expect problems in computing the corresponding coefficient, i.e.

$$\tilde{j}_{N_{MM}} = \frac{\tilde{e}_{N_{MM}}}{s_{N_{MM}}} \tag{16}$$

since $s_{N_{MM}}$ appears as the denominator. Theoretically, the near-zero term in $s_{N_{MM}}$ should cancel with the corresponding term in the numerator.

Following [10], the quantities $s^{-1}_{N_{MM}}$ and $\tilde{e}_{N_{MM}}$ are plotted in Figure 5, as well as the current J_1, which is on the segment nearest the incoming plane wave, and the backscatter RCS, σ, in the vicinity of the lowest interior resonance, $k_0a \approx 2.405$, with $N_{MM} = 32$. As expected, $\tilde{e}_{N_{MM}}$ tends to zero very close to $k_0a \approx 2.405$. However, the peak in $s^{-1}_{N_{MM}}$ is shifted up in frequency. Thus, the cancellation that should occur in the product $s^{-1}_{N_{MM}}\tilde{e}_{N_{MM}}$ is not realized. The anomalies in J_1 and σ are seen to occur at the same value of k_0a as the peak in $s^{-1}_{N_{MM}}$.

The desired current vector can be written as

$$\begin{aligned} \mathbf{J} &= \mathbf{V}\tilde{\mathbf{J}} \\ &= \mathbf{V}\mathbf{S}^{-1}\tilde{\mathbf{E}}_i \end{aligned} \tag{17}$$

and since $\mathbf{V}$ is orthogonal equation (17) can be rewritten as

$$\mathbf{J} = \sum_{n=1}^{N_{MM}} \mathbf{V}_n s_n^{-1} \tilde{e}_n \tag{18}$$

where $\mathbf{V}_n$ is the n-th column of $\mathbf{V}$. With $s_{N_{MM}}$ corresponding to the eigenvalue responsible for the resonance, $\mathbf{V}_{N_{MM}}$ is the basis that supports the resonant mode[2]. Thus, in the MM solution, since $s_{N_{MM}}$ is shifted up in frequency with respect to $\tilde{e}_{N_{MM}}$, the coefficient $s^{-1}_{N_{MM}}\tilde{e}_{N_{MM}}$ of the cavity mode $\mathbf{V}_{N_{MM}}$ in equation (18) is inaccurate in the vicinity of resonance.

For this particular problem, scattering by an infinitely long circular cylinder, more accurate MM matrix elements can be computed with relative ease by modelling the pulse basis functions on segments of the actual, curved, circular cylinder and performing a careful numerical integration. Canning did this in [10] and demonstrated that the shift in frequency of the smallest singular value can be reduced quite substantially. This resulted in a much narrower, in terms of k_0a, anomaly in the current and the disappearance of the anomaly in the RCS. Canning also showed that the condition number increased with the more accurate matrix elements which emphasized that the problem is not due solely to the ill-conditioned matrix since the more ill-conditioned matrix gave more accurate results. Further, since Canning used the same number of unknowns in the computation with more accurate matrix elements as with the less accurate elements, it can be concluded, at least for the circular cylinder considered, that the problem is not entirely due to "truncation error" – the error due to in-

[2]This is easily verified by comparing $\mathbf{V}_{N_{MM}}$ to combinations of the $+n$ and $-n$ terms of the summation in equation (5-109) of [13]. When $J_n(k_0a) = 0$, these terms are cavity mode currents

troducing a finite number of basis and testing functions and thereby reducing the integral equation to a matrix equation [10] – but at least in part due to "numerical error" – approximations made in calculating the matrix elements in terms of the basis and testing functions [10].

4 Protecting the EFIE using the SVD

In the previous section the amount of the resonant current was not computed accurately in the vicinity of an internal resonance. Furthermore, the computed resonant current should in theory not contribute to the scattered field at the resonance frequency. The cavity mode current is represented by the column of $\mathbf{V}$ of the SVD which corresponds to the smallest singular value, i.e. $\mathbf{V}_{N_{MM}}$. As suggested by Canning in [10], the scattered field could be calculated accurately by discarding the resonant current in the vicinity of its resonant frequency. If the MM equation is being solved via the SVD, the mode is easily discarded by setting $s_{N_{MM}}^{-1}$ to zero in equation (18).

Unfortunately the SVD is computationally expensive and operates on a fully square matrix – thus any advantage is lost if the impedance matrix $\mathbf{Z}$ is symmetric. In [7], Canning proposed a method of performing the correction to the current in which the vector $\mathbf{V}_{N_{MM}}$ and the smallest singular value $s_{N_{MM}}$ are approximated by an iterative technique known as the power method (PM). The desired current $\mathbf{J}$ is approximated by orthogonalizing $\mathbf{J}_0$, the current computed directly by the MM, to the resonant mode $\mathbf{V}_{N_{MM}}$ using the formula

$$\mathbf{J} = \mathbf{J}_0 - \mathbf{V}_{N_{MM}} \frac{< \mathbf{V}_{N_{MM}}, \mathbf{J}_0 >}{< \mathbf{V}_{N_{MM}}, \mathbf{V}_{N_{MM}} >} \qquad (19)$$

where $< \mathbf{P}, \mathbf{Q} >$ is a vector inner product in which one takes the complex conjugate of the first vector. In the vicinity of an interior resonance the PM converges rapidly [7].

For the infinitely long circular PEC cylinder, the smallest singular value approximated by the PM is compared with the smallest singular value computed directly by the SVD in Figure 6. The current $\mathbf{J}_0$ was used as the starting vector in the PM and at each frequency the PM was terminated once either the difference between consecutive approximations of the smallest singular value was less than 10^{-8} or 21 iterations had been completed. The approximated value were found to converge quickly, i.e. within 5 iterations, to the exact value in the vicinity of an interior resonance, that is when the smallest singular value corresponds to the eigenvalue responsible for the resonance. Away from resonances, however, the convergence is generally poor and the approximated

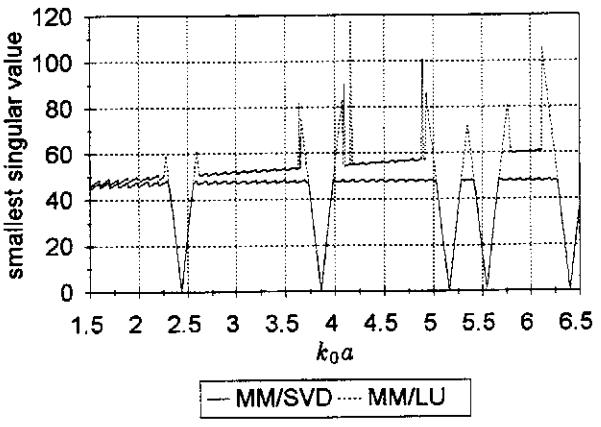

Figure 6: Smallest singular value $s_{N_{MM}}$, exact and approximated, of the MM impedance matrix versus k_0a for a PEC circular cylinder of infinite length. The curve "MM/SVD" is $s_{N_{MM}}$ computed by the SVD while the curve "MM/LU" is $s_{N_{MM}}$ approximated via the power method. The number of unknowns N_{MM} satisfied equation (12).

value is larger – this does not necessarily have a negative consequence since it is still clear from the approximated values where the resonances occur.

Oddly, as a resonance is approached, the power method converges, within at most 20 iterations, prematurely to the mode responsible for that resonance , i.e. before the singular value corresponding with this mode is the smallest one[3]. This accounts for the sudden increase in the approximated smallest singular value as a resonance is approached.

The wavy nature of the curves away from resonance is probably due to the variation in number of unknowns N_{MM} with frequency.

The interior resonances coincide with frequencies where the smallest singular value becomes small, so this could be used as an indication of the occurrence of problems. But, the question is how small should this singular value be in order to know whether to discard the offending current mode? For the problem involving TM scattering by a PEC circular cylinder of infinite length, this question is easily answered if a frequency sweep is carried out. Then, by observing where the anomalies begin and end, with increasing k_0a, in the current or RCS (for example Figure 3), one can determine the value of the smallest singular value at these frequency points from, for example, Figure 6. A threshold can then be derived and the resonant current mode discarded at all frequencies where the smallest singular value is below this threshold. It is also easy to know beforehand where

[3]This may be due to the choice of starting vector

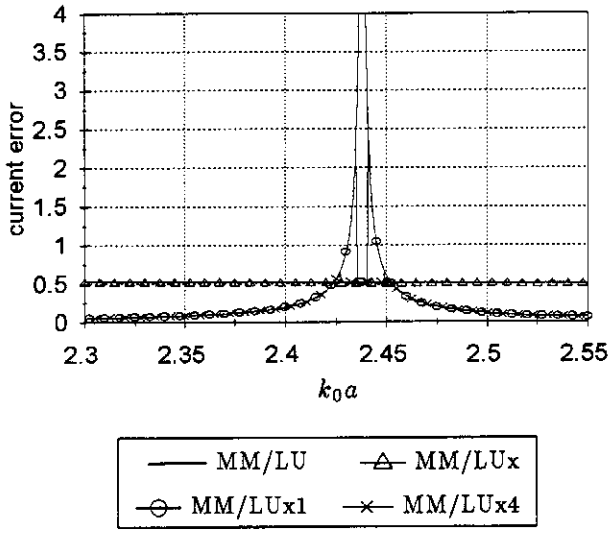

Figure 7: Electric current error Δ_C, without and with current correction versus k_0a in the region of the lowest resonance in the MM solution, computed via the LU decomposition, of a PEC circular cylinder of infinite length excited by an incident TM plane wave. The curve "MM/LU" is with no correction, the curve "MM/LUx" is with equation (19) applied for all k_0a and the curves "MM/LUx1" and "MM/LUx4" are with equation (19) applied where $s_{N_{MM}} \leq 1$ and $s_{N_{MM}} \leq 4$ respectively. The number of unknowns N_{MM} satisfied equation (12). (Maximum in the curve "MM/LU" is approximately 36, off the scale of this figure.)

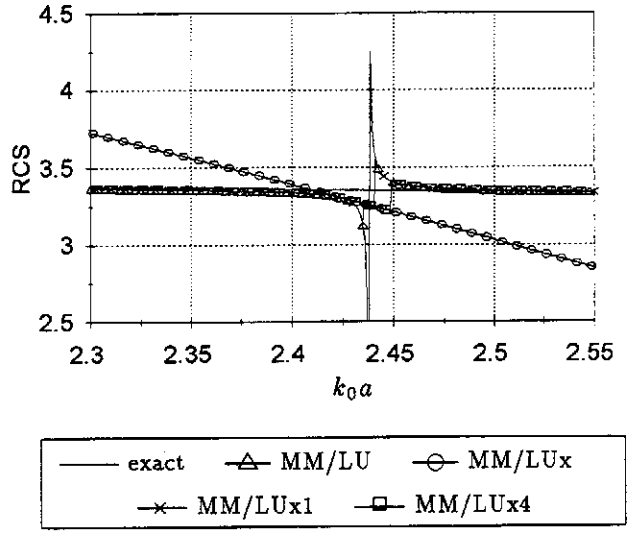

Figure 8: Backscatter RCS, without and with current correction, versus k_0a in the region of the lowest resonance for a PEC circular cylinder of infinite length excited by an incident TM plane wave. The curve "exact" was computed by the Fourier series of equation (3) with equation (6). The remaining curves correspond with those of Figure 7.

to expect the interior resonances to occur as analytical formulas exist for the circular cylinder. However, for a more general problem for which analytical solutions do not exist, it may be extremely difficult or impossible to determine where interior resonances may occur before carrying out the MM solution. Also, if the solution is only desired at a specific frequency and it is computationally expensive to compute a frequency sweep, how does one know what the threshold in smallest singular value should be? How dependent is this threshold on the geometry of the problem being solved?

Three possibilities were investigated and their effect on the current error is compared in Figure 7 and on the backscatter RCS in Figure 8.

The first was to discard $\mathbf{V}_{N_{MM}}$ at all frequencies. This seems feasible since away from resonance this vector corresponds to a higher order term in the series expansion, equation (3), of the exact solution which does not make a significant contribution. The anomaly in Δ_C has been suppressed but the error is now increased over the whole range of k_0a where $s_{N_{MM}}$ corresponds to Λ_0. The latter situation is because the mode represented by $\mathbf{V}_{N_{MM}}$ has been completely removed while part of it should be contributing to the desired solution for the current even at the precise resonance point and for the scattered field except at the precise resonance point. The current error Δ_C remains constant over the whole range of k_0a where $s_{N_{MM}}$ corresponds to Λ_0. It is constant here because the exact current contains a constant amount of $V_{N_{MM}}$. There is also a large improvement in the backscatter RCS where the anomaly occurred. However, the deviation becomes larger with decreasing or increasing k_0a away from this point, emphasizing that it is inappropriate to carry out the orthogonalization away from the resonance point and that it is thus important that the resonances be detected.

It is evident from Figures 7 and 8 that one cannot expect to completely solve the problem by suppressing $\mathbf{V}_{N_{MM}}$, however, the anomalies can be drastically reduced. Ideally, away from the anomalies one would like to retain the solution without $\mathbf{V}_{N_{MM}}$ discarded. This was attempted by setting a threshold in $s_{N_{MM}}$ and only discarding $\mathbf{V}_{N_{MM}}$ when $s_{N_{MM}}$ is beneath it. The effect on Δ_C for two thresholds, $s_{N_{MM}} \leq 1$ and $s_{N_{MM}} \leq 4$, is also plotted in Figure 7. These values were arrived at by observing $s_{N_{MM}}$ in the vicinity of the anomalies using Figures 3 to 4. A threshold of 4 brings the error down to almost the best that can be achieved while a threshold of 1 is a bit low, although the anomaly is drastically suppressed.

The backscatter RCS for $S_{N_{MM}}$ with these thresholds

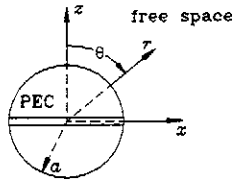

Figure 9: A PEC sphere with a rotationally symmetric equatorial aperture.

is plotted in Figure 8. With the threshold of 1 the maximum deviation in the RCS from the exact solution is about 10% while with a threshold of 4 it is about 4%.

5 Protecting the MM/BOR formulation from interior resonances

In this section the application of Canning's method, presented in [7], to the MM/BOR formulation for the solution of scattering [8] and radiation [9] from composite bodies of revolution is discussed. For penetrable regions the MM/BOR formulation uses the CFIE. However, for conducting regions the EFIE is used which results in a complex symmetric impedance matrix (this would not be the case if the CFIE was used for conducting regions as well). Thus, for problems involving conducting regions, the MM/BOR formulation can suffer from the interior resonance problem.

The method's application is demonstrated here for two problems that can also be solved analytically: firstly, radiation from a rotationally symmetric aperture in a PEC sphere, and secondly, the same problem with the PEC sphere covered by a spherical dielectric shell.

5.1 Radiation from a rotationally symmetric equatorial aperture in a PEC sphere

The problem is illustrated in Figure 9. The PEC sphere has a of radius 100 mm and has a rotationally symmetric aperture at its equator. The aperture subtends an angle of 5° in θ and it is assumed that only a θ-directed electric field exists in the aperture. This excitation will produce fields TM to the radial direction. The electric field is constant across the aperture, i.e. a pulse distribution in θ.

An analytical solution for this problem, in terms of a spherical wave function expansion (SWFE), is presented by Harrington in [13, pages 301-303] for the case where the aperture has a small width so that the aperture field is an impulse function in θ. This solution can easily be

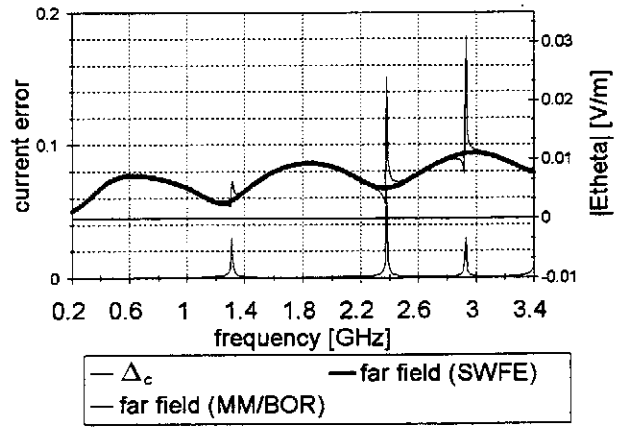

Figure 10: Electric current error Δ_C and the far field, at $\theta = 90°$, in the MM solution of radiation from a rotationally symmetric equatorial aperture in a PEC sphere of radius 100 mm. The number of unknowns provided ten basis functions per wavelength at 3.4 GHz.

modified to solve problems involving an aperture subtending an arbitrary angle in θ [9, Appendix D].

For the radiation problems presented here, the current error is defined as

$$\Delta_C = \sqrt{\frac{\iint_S |\vec{J}_{MM} - \vec{J}_{SWFE}|^2 \, ds}{\iint_S ds}}. \qquad (20)$$

where $\vec{J}_{MM}$ is the current computed by the MM, S is the outer surface of the PEC sphere and $\vec{J}_{SWFE}$ is the current computed by the SWFE using the relationship $\vec{J}_{SWFE} = \hat{r} \times \vec{H}$ where $\hat{r}$ is the unit vector in the r-direction and $\vec{H}$ is the exterior magnetic field.

In Figure 10 the current error in the MM/BOR solution and the radiated far field are plotted from 0.2 to 3.4 GHz. Anomalies occur in the vicinity of resonance frequencies of a spherical cavity [13, pages 269-273].

The smallest singular value approximated using the PM is compared with that computed directly by the SVD in Figure 11. The behaviour of the approximated smallest singular value is similar to that in the problem involving the PEC cylinder (see Figure 6) in that it also converges to the singular value corresponding to the resonant mode away from the resonance as well as at the resonance. As was the case in the PEC cylinder problem, the PM converges to the singular value corresponding to the resonant mode prematurely, i.e. before it is actually the smallest singular value, which results in a sudden increase in the approximated value.

A further observation is that the smallest singular value computed directly by the SVD increases gradually with frequency outside of the resonance region and does not remain approximately constant as was the case

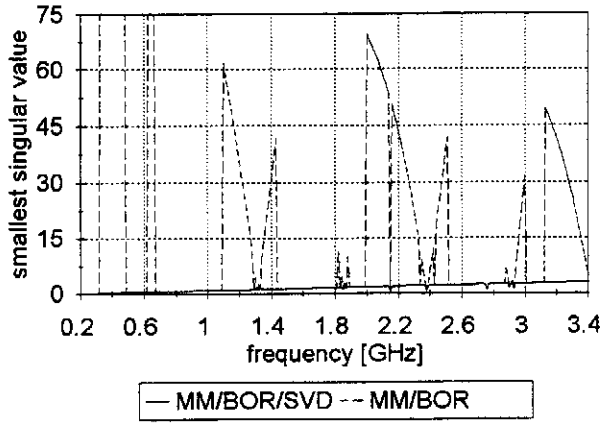

Figure 11: Smallest singular value $s_{N_{MM}}$ of the MM impedance matrix for a PEC sphere of radius 100 mm. The curve "MM/BOR/SVD" is $s_{N_{MM}}$ computed by the SVD while the curve "MM/BOR" is $s_{N_{MM}}$ approximated via the power method. The number of unknowns provided ten basis functions per wavelength at 3.4 GHz.

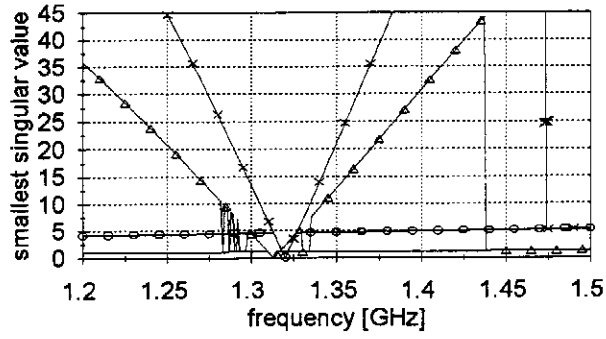

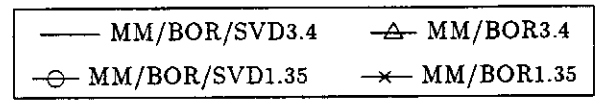

Figure 12: Smallest singular value $s_{N_{MM}}$ of the MM impedance matrix for a PEC sphere of radius 100 mm in the vicinity of the lowest interior resonance. The curves "MM/BOR/SVD3.4" and "MM/BOR/SVD1.35" are $s_{N_{MM}}$ computed by the SVD while the curves "MM/BOR3.4" and "MM/BOR1.35" are $s_{N_{MM}}$ approximated via the power method. The numbers in the labels, i.e. 3.4 and 1.35, refer to the frequency in GHz at which the discretization used to compute the curves provided ten basis functions per wavelength.

in the results for the problem involving a PEC circular cylinder (see Figure 4 or 6). The difference here is that the number of unknowns is kept constant, providing ten basis functions per wavelength at 3.4 GHz, whereas in the PEC cylinder computations the number of unknowns was varied with frequency.

It is difficult to determine a suitable smallest singular value threshold from Figure 11 for carrying out the current correction. If one is to carry out the correction across the entire frequency range displayed then the threshold must always be beneath the smallest singular value away from resonance. However, if this is satisfied at the lower frequencies, the resonances at the higher frequencies will not be detected. This problem can possibly be avoided by varying the discretization with frequency, so that there are just ten unknowns per wavelength at each frequency, as was done in Figure 6. Then, away from resonances, the smallest singular value should be larger in magnitude and remain more constant with frequency. Unfortunately, the computer implementation of the MM/BOR method was not at a point where this could readily be done at the time of writing this paper.

In Figure 12 the smallest singular value is plotted in the vicinity of the first interior resonance using two discretizations. The first is as above, which provided ten unknowns per wavelength at 3.4 GHz, and the second provided ten unknowns per wavelength at 1.35 GHz. Indeed, for the coarser discretization, which is sufficient at the resonance, both the exact and approximated singular values are larger. The resonance frequency is also shifted up in frequency due to the increased truncation error.

Using the curves of the coarser discretization a threshold of 4 in the approximated smallest singular value was chosen to carry out the correction on the current. The current error obtained using equation (19) with the PM at all frequencies as well as with the threshold of $S_{N_{MM}} = 4$ are plotted in Figure 13, as the curves "MM/BORx" and "MM/BORx4" respectively, along with the original current error, the curve "MM/BOR", in the vicinity of the lowest resonance. The anomaly is completely suppressed for the correction at all frequencies ("MM/BORx") and in contrast to the results for scattering by the PEC circular cylinder, see Figure 7, the error is now small at all frequencies. The result is also good with the threshold of 4 ("MM/BORx4").

Far field results at $\theta = 90°$ achieved with the correction at all frequencies, the curve "MM/BORx", with the threshold of 4, the curve "MM/BORx4", and with a threshold of 15, the curve "MM/BORx15", are compared in Figure 14 to the far field computed by the MM/BOR method without correction as well as the SWFE solution. The result obtained with the correction at all frequencies (MM/BORx) is excellent at frequencies below resonance and at the resonance the anomaly is completely suppressed. However, above the resonance

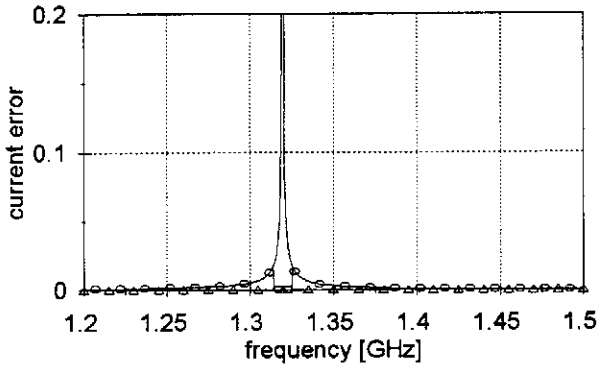

Figure 13: Electric current error Δ_C in the region of the lowest resonance in the MM solution of radiation from a rotationally symmetric equatorial aperture in a PEC sphere of radius 100 mm. The curve "MM/BOR" is with no correction and the curves "MM/BORx" and "MM/BORx4" are with equation (19) applied at all frequencies and at frequencies where $s_{N_{MM}} \leq 4$ respectively. The number of unknowns provided ten basis functions per wavelength at 1.35 GHz.

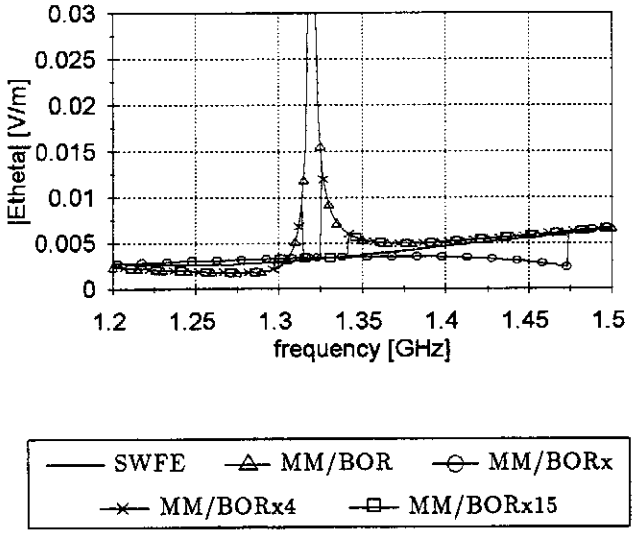

Figure 14: Far field, at $\theta = 90°$, in the region of the lowest resonance of the rotationally symmetric equatorial aperture in a PEC sphere of radius 100 mm computed by the SWFE and the MM. The curve "SWFE" is the SWFE solution, curves "MM/BORx" and "MM/BORx4" correspond to those of Figure 13 and "MM/BORx15" is with a threshold of 15.

this result increasingly deviates with frequency until 1.475 GHz where it jumps to the correct solution. This is the frequency at which the approximated smallest singular value converges to the exact smallest singular value (see Figure 12). With a threshold of 4 the anomaly is reduced drastically in close proximity to the resonance but slightly away the deviation is still relatively large. A far better result is achieved with a threshold of 15 which also does not alter the solution above 1.475 GHz.

From the above results it appears that the current correction procedure using the PM can safely be used at all frequencies where the approximated smallest singular value has converged to the actual smallest singular value – this can be at and in close proximity to the resonant frequency as well as away from resonances. The reason for this is that at a resonance the smallest singular value corresponds to the undesired mode that must be thrown away and away from resonance the smallest singular value corresponds to a mode whose contribution is small if the discretization is sufficiently fine. It is not safe, however, to carry out the current correction at those frequencies at which the approximated smallest singular value is not the actual smallest singular value as the approximated value then corresponds to a mode that makes a desired and necessary contribution.

The problem remains as to how to determine at a discrete frequency, without having done a frequency sweep, whether a resonance occurs especially for a complex geometry. It is evident from the above results that the problem is made a bit easier if the number of unknowns in the solution is just sufficient at that frequency. However, a knowledge of the magnitude of the smallest singular value away from resonance still appears to be necessary.

5.2 Radiation from a rotationally symmetric equatorial aperture in a PEC sphere with a spherical dielectric shell.

This problem is illustrated in Figure 15. An analytical solution, in terms of a spherical wave function expansion (SWFE) [9, Appendix D], can be derived using the methods presented in [13, Chapter 6].

The radius of the PEC sphere is 100 mm and the outer radius of the dielectric shell is 150 mm. The dielectric shell has a relative permittivity $\epsilon_r = 3$ and relative permeability $\mu_r = 1$. As for the problem without the shell, the aperture subtends an angle of 5° in θ and it is assumed that only a θ directed electric field exists in the aperture.

The current error in the MM solution for this problem and the radiated far field are plotted in Figure 16. The interior resonances of the sphere have shifted down in

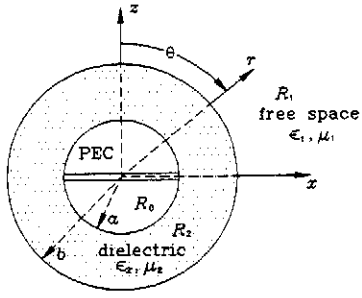

Figure 15: A PEC sphere, coated by a spherical dielectric shell, containing a rotationally symmetric equatorial aperture.

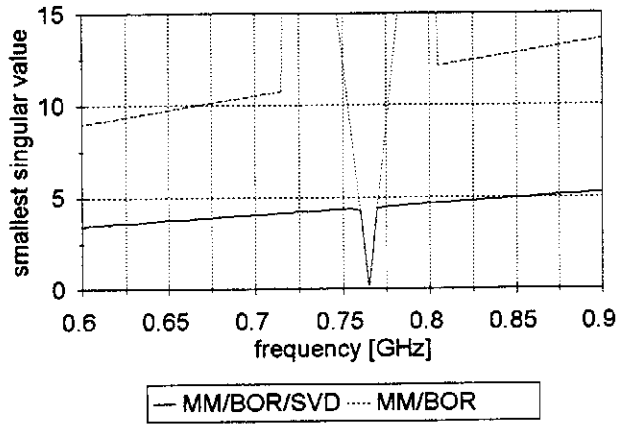

Figure 17: Smallest singular value $s_{N_{MM}}$, in the frequency range 0.6 to 1 GHz, of the MM impedance matrix for a PEC sphere of radius 100 mm with a spherical dielectric shell of radius 150 mm and relative permittivity $\epsilon_r = 3$. The curve "MM/BOR/SVD" is $s_{N_{MM}}$ computed by the SVD while the curve "MM/BOR" is $s_{N_{MM}}$ approximated via the power method. The number of unknowns provided ten basis functions per wavelength at 0.9 GHz.

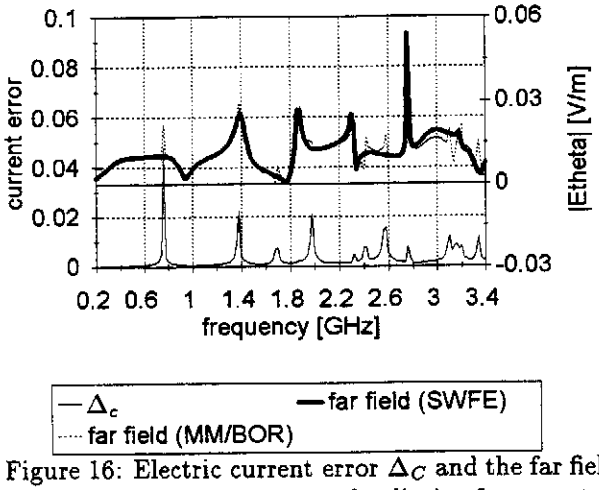

Figure 16: Electric current error Δ_C and the far field, at $\theta = 90°$, in the MM solution of radiation from a rotationally symmetric equatorial aperture in a PEC sphere of radius 100 mm with a spherical dielectric shell of radius 150 mm and relative permittivity $\epsilon_r = 3$. The number of unknowns provided ten basis functions per wavelength at 3.4 GHz.

frequency, as is evident in the positions of the anomalies in the current error, due to the presence of the shell. This is a result of the application of the equivalence principle in the formulation of the EFIE which replaces the interior region with the same material as the surroundings. This also means that there are now more interior resonances in the frequency range shown as some of the higher resonances have shifted down.

It is clear that not all the apparent anomalies in the far field are due to interior resonances as they are also present in the result computed by the SWFE. Some of the anomalies due to interior resonances have merged with actual anomalies in the result computed via the MM/BOR formulation. Thus, the presence of an anomaly in the frequency sweep of a quantity such as the far field is not necessarily an indication of an interior resonance.

The smallest singular value for this problem in frequency subrange 0.6 to 1 GHz is plotted in Figure 17.

Inspection of Figure 17 led to a threshold of 8 being applied to the current orthogonalization procedure in the frequency range 0.6 to 1 GHz. The resultant change in current error is shown in Figure 18 and the change in the field in Figure 19. From these figures it is seen that the method does work; however the problems regarding the detection of interior resonances remain.

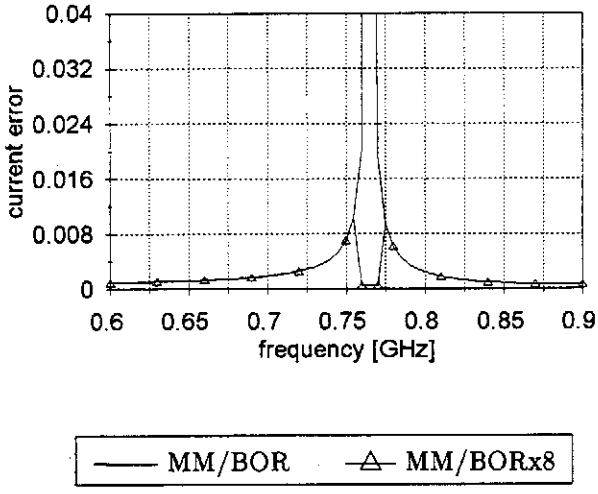

Figure 18: Electric current error Δ_C in the frequency range 0.6 to 0.9 GHz in the MM solution of radiation from a rotationally symmetric equatorial aperture in a PEC sphere of radius 100 mm with a spherical dielectric shell of radius 150 mm and relative permittivity $\epsilon_r = 3$. The curve "MM/BOR" is with no correction and the curve "MM/BORx8" is with equation (19) applied at frequencies where $s_{N_{MM}} \leq 8$. The number of unknowns provided ten basis functions per wavelength at 0.9 GHz.

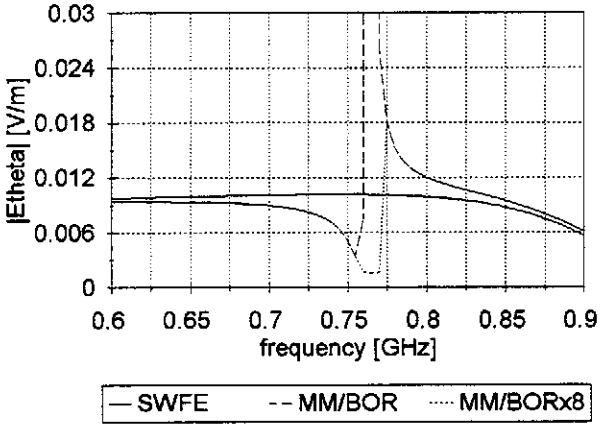

Figure 19: Far field in the frequency range 0.6 to 0.9 GHz, at $\theta = 90°$, of the rotationally symmetric equatorial aperture in a PEC sphere of radius 100 mm with a spherical dielectric shell of radius 150 mm and relative permittivity $\epsilon_r = 3$ computed by the SWFE and the MM. The curve "SWFE" is computed via the SWFE while the remaining curves correspond with those of Figure 18.

6 Conclusions

The electric field integral equation, which is a surface integral equation, is valid for both the exterior and interior problems as defined in section 1. Although the interior solution should not couple to the exterior solution and vice versa in theory, when solving numerically, anomalies are observed at discrete frequencies that coincide with the eigenfrequencies of the interior solution. This is a well-known result in the literature and is demonstrated here.

A comparison between an analytical solution and a moment method solution for a canonical problem shows how the interior resonance problem arises. In the analytical solution for the electric current, the eigenvector corresponding to the zero eigenvalue is generally present but does not radiate any external field. However, with the aid of the singular value decomposition (SVD), it is seen that in the approximate moment method solution the zero in the eigenvalue, or smallest singular value, shifts in frequency with respect to the zero in the excitation thus the quotient in equation (16), which is the coefficient of the eigenvector corresponding to the zero eigenvalue, is inaccurate. Canning has demonstrated that the problem may be more due to approximations made in calculating the matrix elements in terms of the basis and testing functions, than due to introducing a finite number of basis and testing functions.

The anomalies in the computed results for the exterior field can be suppressed by discarding the eigenvector corresponding to the smallest singular value in the vicinity of an interior resonance. This was demonstrated using the singular value decomposition to solve the moment method matrix equation directly as well as by using the power method to approximate the smallest singular value and the corresponding eigenvector. It was found that the eigenvector corresponding to the smallest singular value can safely be discarded at all frequencies, provided a sufficient number of unknowns is used, as at an interior resonance it makes an undesired contribution and away from resonance its contribution is small. However, the power method does not always converge to the smallest singular value but converges to the eigenvector responsible for a resonance prematurely.

The question still remains on how to detect the occurrence of such resonances in a foolproof manner. The detection is easy for canonical problems as analytical formulas exist for the eigenvalues. However, for general problems the size of the smallest singular value depends on the geometry of the problem. A possible way around this is to do a frequency sweep if it is suspected that an interior resonance is present. However, this could prove computationally very expensive and, it was demonstrated that anomalies in the computed results do

not necessarily indicate interior resonances. More work needs to be done to find a reliable method, if possible, of detecting interior resonances that takes the geometry of the problem into account.

The major contribution of the work presented in this paper is the demonstration that whilst the method used to avoid the interior resonances can work, applying it automatically in a MM code is not as straightforward as was implied by Canning [7]. The major obstacle is that the power method only converges to the smallest singular value in the region of resonance. This has been illustrated in this paper using a number of examples, including rotationally symmetric radiators. The full SVD is unfortunately very expensive computationally, making the direct use thereof most unattractive. A further contribution is the specific investigation of the method with regard to the MM/BOR solution of radiation problems.

Acknowledgements

We gratefully acknowledge the most helpful comments of Dr. Joseph R. Mautz, who drew our attention to several errors in the draft version of this paper.

References

[1] J. R. Mautz and R. F. Harrington, "H-field, E-field, and combined-field solutions for conducting bodies of revolution," *AEU*, vol. 32, pp. 157–164, 1978.

[2] J. R. Mautz and R. F. Harrington, "A combined-source solution for radiation and scattering from a perfectly conducting body," *IEEE Trans. Antennas Propagat.*, vol. AP-27, pp. 445–454, July 1979.

[3] L. N. Medgyesi-Mitschang and D.-S. Wang, "Hybrid solutions for scattering from perfectly conducting bodies of revolution," *IEEE Trans. Antennas Propagat.*, vol. AP-31, pp. 570–583, July 1983.

[4] L. N. Medgyesi-Mitschang and J. M. Putnam, "Integral equation formulations for imperfectly conducting scatterers," *IEEE Trans. Antennas Propagat.*, vol. AP-33, pp. 206–214, February 1985.

[5] P. L. Huddleston, L. N. Medgyesi-Mitschang, and J. M. Putnam, "Combined field integral equation formulation for scattering by dielectrically coated conducting bodies," *IEEE Trans. Antennas Propagat.*, vol. AP-34, pp. 510–520, April 1986.

[6] A. F. Peterson, "The "interior resonance" problem associated with surface integral equations of electromagnetics: numerical consequences and a survey of remedies," *Electromagnetics*, vol. 10, pp. 293–312, 1990.

[7] F. X. Canning, "Protecting EFIE-based scattering computations from effects of interior resonances," *IEEE Trans. Antennas Propagat.*, vol. 39, pp. 1545–1552, November 1991.

[8] L. N. Medgyesi-Mitschang and J. M. Putnam, "Electromagnetic scattering from axially inhomogeneous bodies of revolution," *IEEE Trans. Antennas Propagat.*, vol. AP-32, pp. 797–806, August 1984.

[9] P. Steyn, *A Moment Method Solution of Electromagnetic Radiation from Composite Bodies of Revolution*. PhD thesis, University of Stellenbosch, South Africa, November 1994.

[10] F. X. Canning, "Singular value decomposition of integral equations of EM and applications to the cavity resonance problem," *IEEE Trans. Antennas Propagat.*, vol. 37, pp. 1156–1163, September 1989.

[11] R. F. Harrington, *Field Computation by Moment Methods*. Malabar, Florida: Robert E. Krieger, first ed., 1982. Reprint of 1968 edition.

[12] G. H. Golub and C. F. van Loan, *Matrix Computations*. Baltimore, Maryland: The John Hopkins University Press, first ed., 1983.

[13] R. F. Harrington, *Time-Harmonic Electromagnetic Fields*. New York: McGraw-Hill, first ed., 1961.

The authors

Pierre Steyn was born in Cape Town, South Africa in 1962. He received the Bachelor and Master degrees in electronic engineering (both cum laude) from the University of Stellenbosch, South Africa in 1986 and 1989 respectively. In 1994 he received the Ph.D. degree in Electronic Engineering from the University of Stellenbosch. His chief research interests are in computational electromagnetics and computer aided antenna design. Pierre is presently persuing a career in commercial antenna design.

David Bruce Davidson: See biography elsewhere in this issue.